International Research Journal of Engineering and Technology (IRJET) e-ISSN: 2395-0056
Volume: 07 Issue: 05 | May 2020 www.irjet.net p-ISSN: 2395-0072

Active Front-End Converter Design for the On-Board Charger in Electric Vehicles

K Anusha[1], Vasu M[2], Dr. Anitha G S[3]

[1]*PG Student, Department of Electrical and Electronics Engineering, RV College of Engineering, Bengaluru*
[2]*Architect Transportation Department, L&T Technology Services, Bengaluru*
[3]*Associate Professor, Department of Electrical and Electronics Engineering, RV College of Engineering, Bengaluru*

***

Abstract - *As the world is gearing up to unleash an EV revolution, it is still true that the rate of adaption is slow. Electric Vehicles (EVs) despite being a greener, smoother and cheaper mode of transport does not seem to be practical yet. The reason is two words, Cost and Ecosystem. Currently EV's are priced substantially at par with Gasoline cars making it a less significant choice for buyers, the advancement in battery technology and government schemes are expected to bring down the cost of EV in future. The objective of the work is to design an OBC to charge a battery of 6.6kW for EV. This charger controls the values of the output voltage and current and maintains them at a value as desired. A first converter (active front-end converter) is used to convert the grid supply of 230V, 50Hz to DC of 400V. A second converter (bi-directional bridge converter) adjusts the DC output to the level battery requires and it also provides isolation between grid and vehicle battery. The control of the AFC is comprehended by using a PFC function. This reduces the impact on the grid during peak demand. And this high efficiency electric vehicle can be used as immediate alternate solution for conventional vehicle.*

Keywords* – *Electric vehicle (EV), active front-end converter (AFC), active power decoupling (APD), DC-to-DC converter, totem-pole, interleaved boost converter, synchronous rectification, on-board charger (OBC).

1. INTRODUCTION

Two major challenges human civilization is facing these days are energy and environment. Nowadays, energy prices have also been rising and public opinion on environmental protection is increasing. Rules and regulations have also become rigorous, "emission reduction" and "energy saving" has become crucial genuine problem. Hence, use of new technology to reduce energy consumption and reduction has become an important direction in the development of the automobile industry, and electric vehicle has become an attractive solution for energy saving and reduction in emission. EV is attributed in two simple points as: EV solves the problem of environmental pollution. And EV helps to get rid of dependence on petroleum resources. Electric vehicles contain traction batteries, whose voltages are typically about 300-400V. The architecture of EV is shown in Fig. 1.

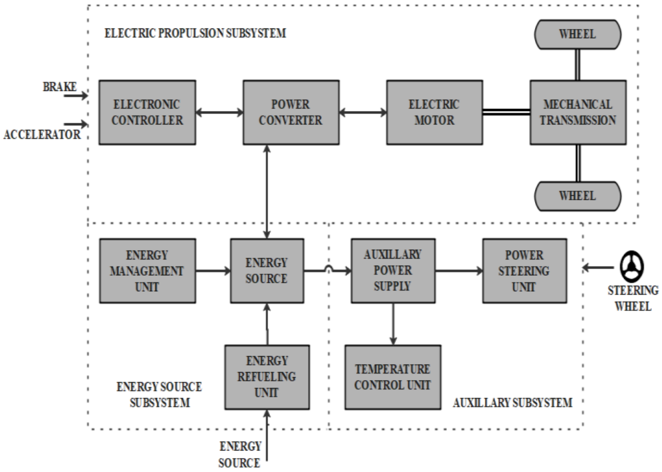

Fig.1: General Architecture of EV.

The process of charging the EV refers to the electronic communication between the EV battery and the grid power supply. The purpose is to avoid overloading and to confirm safety. There are various kinds of energy storage systems (batteries). Li-ion batteries have highest energy-density and low self-discharging rate, compared to other batteries, and hence, has a potential world market [1]. Li-ion storage cell are generally functional in EVs because of their light weight. EVs uses grid supply to charge the batteries. OBC's allow users to charge their EV batteries wherever there is an availability of electric power channel [2]. The EV battery is charged only when the car is at standstill, except for regeneration at decelerating, so, using the on-board traction system components to form an unified charging device is made possible.

1.1 On-Board Charger

On-board charger is a part of the EV, as depicted in the Fig. 2. It allows charging at every place possible as long as the supply, either 1-ph or 3-ph, is available. The use of the OBC improves the charging convenience of the vehicle. The main disadvantage of this structure is additional DC-to-AC inverter is required.

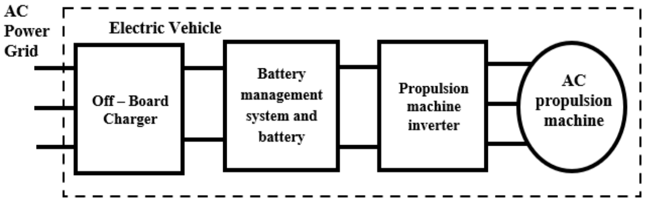

Fig.2: General Block Diagram of OBC.

1.2 Block Diagram of OBC

The main objective of the OBC is to charge-up the traction battery. OBC architecture proposed for the electric vehicles is shown in Fig. 3. The on-board charger is made of three functional modules.

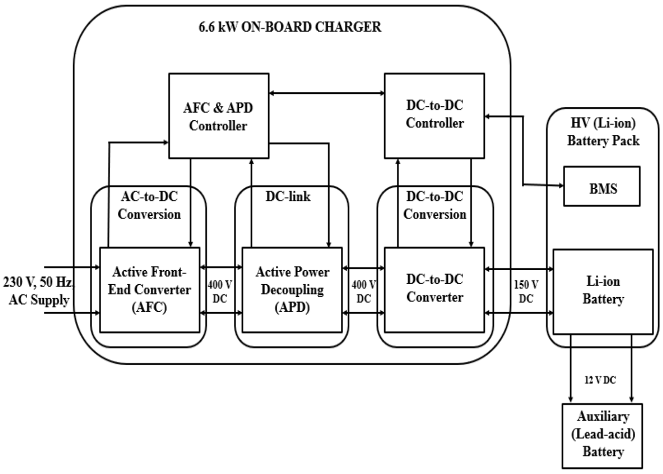

Fig.3: Block Diagram of Proposed OBC for EV.

The OBC is designed to serve the following functions:

- Converting AC quantities from the grid into DC quantities that charges the vehicle's battery.
- Providing power factor correction (PFC) to shape the input current to a power supply, maximizing efficiency and reducing harmonics.
- Adjusting the produced DC voltage up or down to provide the correct DC levels to the battery.
- Auxiliary battery is charged from the main battery for the auxiliary loads in the electric vehicle.

1.3 Active Front-End Converter

On-Board Battery Chargers (OBC) actually have three important modules, they are Active Front-end Converters (AFC), Active Power Decoupling (APD) Circuit, and a dc-to-dc converter. Active Front-end Converter converts ac-to-dc or vice versa. Typically, in plug-in electric vehicle (PEV), a 1-ph PFC bridge converter is implemented as first stage of OBC, then an isolated dc-to-dc converter as the next stage [3]. But by the use of conventional circuits efficiency is less. Then, the most generally employed converter in an OBC is a 1-ph diode-bridge ac-to-dc converter circuit followed by a dc-to-dc converter. It alters the 1-ph grid ac quantities to a regulated dc voltage [4]. But the converters used were unidirectional that serves from grid to vehicle only. Semi-boost bridgeless PFC converter were used, which were slightly modified to operation in vehicle to grid mode. And it also reduced the common mode noise. But each bridge had to bear the maximum input current, leads to increase in the dimensions and thereby cost of the components [5]. A bi-directional bridge-less totem-pole interleaved PFC converter by means of MOSFETs as first step of an OBC for EVs is proposed in this project. The projected converter offers bi-directional operation, permitting both G2V mode and V2G auxiliary services. This converter is appropriate for effective bi-directional on-board charging due to its advantages with respect to bi-directional action, reduced current ripple, lesser EMI, low switching losses and conduction losses [6].

The output of this active front end converter is desired to be with less ripple which is then utilized by the converter for further operation of OBC. The converter which converts AC power supply to the DC power supply is called as rectifier. The most commonly used rectifier is the diode bridge rectifier. One of the major concerns about selecting the topology of the rectifier is the harmonic in the line currents due to the source inductance. These harmonic components are responsible for the distortion of the voltage at the point of common coupling and produce undesirable effects. Due to which power factor becomes worst. Hence Power Factor Correction (PFC) is implemented using parallel switching devices, interleaved PFC, and bridgeless PFC that provides even higher efficiency.

1.4 Block Diagram of AFC

AFC converts the AC power supply to the DC supply as required by the battery. AFC has a controller that controls the circuit operation. Fig.4 show the high-level block diagram of AFC circuit.

Voltage sensing and current sensing circuits sense the voltage level and current level through the circuit and sends the signal to the control. Feedback signals from the temperature sensor, voltage and current measurement are loaded to the controller to monitor the health of the converter. The gating pulses to the switches in the circuit is given by the gate driver circuit. DC-link capacitance of the dc-to-ac converter reduces the ripples. Controller used is of automotive standards with required number of GPIOs, ADCs, and DACs. It constantly monitors the overall operation of the system. Microcontroller has the CAN port that communicates with the BMS (Battery Management System) using CAN controller. The microcontroller provides the necessary control signals to the driver circuit based on the BMS output.

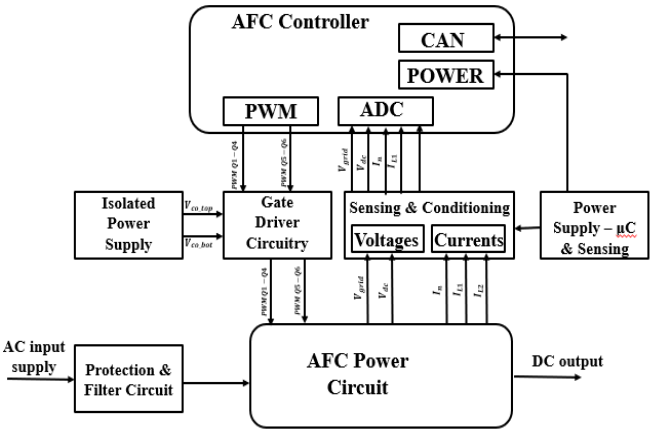

Fig.4: Block Diagram of AFC Circuit.

1.5 Synchronous Rectification

In many applications diodes are used for rectification. Due to the diode conduction losses the overall power loss increases. The conduction losses are high in applications having higher current ratings. The equivalent forward voltage drop of MOSFET is very less compared to diode forward voltage drop. Hence, diodes are replaced by MOSFETs.

2. METHODOLOGY

Active Front – End Converter (AFC) is used to convert the grid supply (230 V, 1- ϕ, 50Hz) to DC (400 V) supply. The topology used is interleaved bridgeless totem – pole. The input current has large harmonic distortion, and it pollutes the grid. Hence PFC circuit is used to reduce the harmonics, and to meet the International standards of power factor and harmonic content requirement.

2.1 Structure

The conventional PFC has the diodes that restricts the bidirectional action of the converter. In this topology, for two-way operation, transistors and diodes operation are included in the rectifier bridge. Hence, the name bridgeless PFC converter. This reduces the number of semiconductor and therefore the conduction losses. And the diodes are replaced by the slow switching Mosfet, enabling the flow of negative current. It now operates in Bidirectional mode. This also helps in synchronous rectification. Interleaving the totem – leg increases the overall efficiency of the converter and reduces the stress on the semiconductor switches. When compared to other mentioned topologies, the converter presented here has advantages of higher efficiency, smaller common mode noise, reduced ripples in ac input current, less reverse recovery current, a smaller no. of elements, simple control and simple gate drive design. Totem-pole bridge-less interleaved converter is as shown in the Fig.5 below. The critical components are:

- Power Switches (S_1 to S_2)
- Filter Inductances (L_1& L_2)
- DC link Capacitance (C_0)

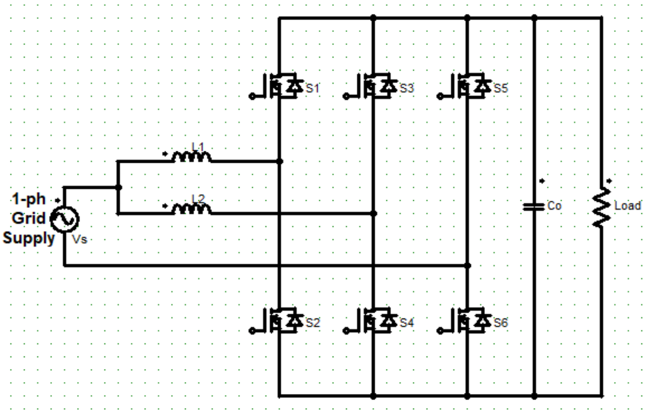

Fig.5: Totem pole Bridgeless Interleaved PFC circuit.

2.3 Operation

Fig.5 shows the proposed bi-directional interleaved bridge-less totem pole PFC converter has six Mosfet. Two interleaved boost converters are reactor L_1, switches S_1 & S_2 and reactor L_2, switches S_3 & S_4 which are operated with phase-shift of 180^0. In every phase, the top switch and the bottom switch operates complementing each other with a short dead-band period. Diodes for line-rectification are substituted with two switches (S_5 and S_6) to be used for synchronous-rectification, this adds to the reduction in power losses and improving efficiency.

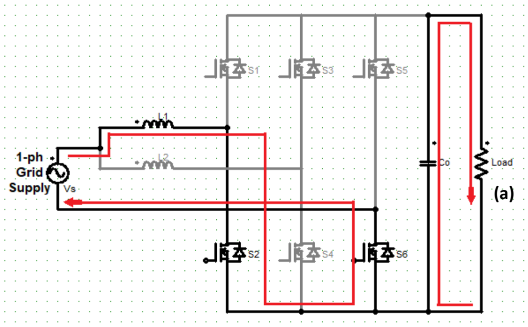

In the first half-period of supply, as seen in Fig.6(a), S_6 is closed, linking the positive side of grid supply to ground. And when S_2 is closed, the inductor L_1 gets charged.

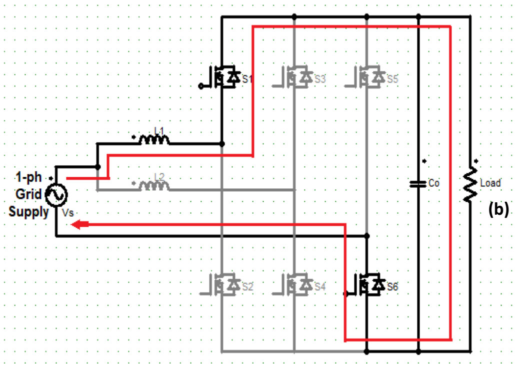

Then S_2 is opened, a dead band period is provided beforehand S_1 is on in order to avoid over-shoot in the current. After the deadband, S_2 is closed, seen in Fig.6(b), creating a free-wheeling path for current through inductor and discharges the stored energy in the dc-link capacitor.

The ON time of S_2 is calculated by the duty cycle of boost converter, whereas the ON time of switch, S_1 is complimentary to S_2.

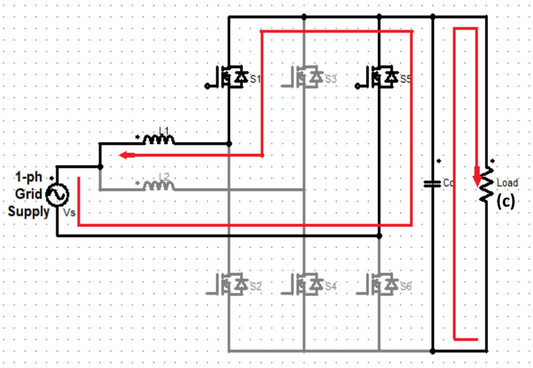

In the second half-period of supply, S_5 is closed, joining the positive side of grid supply to dc-link. Then S_1 is closed, as seen in Fig.6(c), the source charges the reactor L_1.

S_2 is closed after S_1 is opened with a dead-band period, which allows synchronous-rectification and creates a free-wheeling path for current through inductor, as seen in Fig.6(d).

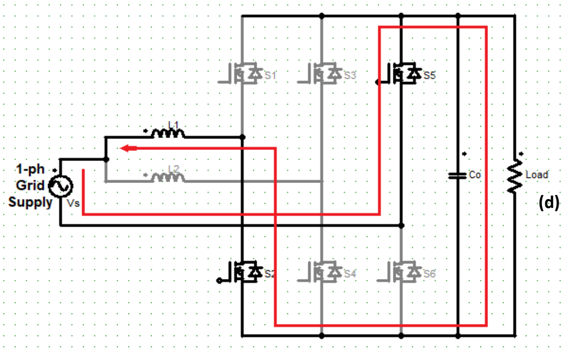

Fig.6: Different Modes of Operation of the Proposed Topology for G2V mode.

In the second half-period of supply, the ON time of switch, S_1 is calculated by dc-to-dc converter duty cycle. Switch S_3 and switch S_4 are used in the other phase, operated with phase-shift of 180^0 in regards with switches S_1 & S_2. The working of other boost interleaved phase is same as that of first phase, improving the effective operating frequency to double.

2.2 Controller

The controller structure of the AFC unit is as shown below in Fig.7. As seen in the Fig.7, there are three controllers or compensators (two current and one voltage) in the control loop. The AFC control loops design consists of the current-loop in the inner side, and the voltage-loop controller outer side. The inner current-loop controllers are fast controllers and the outer voltage-loop controllers are slow controllers.

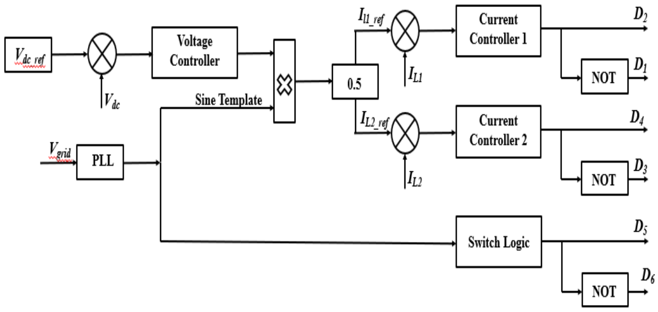

Fig.7: Control Diagram of AFC Circuit.

Initially, the analog approach is followed for the compensator design, where the whole design is made in the continuous-time domain (s-domain). Finally, the parameters of the compensators are converted back into the discrete domain by using Bilinear transformation.

The other important hardware components in the AFC are:

- Driver circuit to provide gate-pulses to the power devices.
- Sensing circuits (current and voltage).
- EMI filters and protection circuit.
- Snubbers across the power devices (if required).

3. DESIGN OF CONVERTER

The most commonly used rectifier is the diode bridge rectifier. One of the major concerns about selecting the topology of the rectifier is the distortions in line current due to the source inductance. These harmonic components are responsible for the distortion of the voltage at the PCC and produce undesirable effects. Due to which power factor becomes worst. The reactors (L_1, L_2) helps improve the power factor and the diodes and smoothing capacitors convert ac-to-dc.

The specifications of the AFC are as follows:

- Input AC Voltage - 230 V
- Output DC Voltage - 400 V
- Output Power - 6.6 kW
- Line Frequency - 50 Hz
- Switching Frequency - 100 kHz
- Maximum DC Voltage - 600 V

And consider,

- Efficiency - 93 %
- Power factor - 0.95

3.1 Inductor Calculation

Input Current is given as,

$$I_{in\_rms} = \frac{P_{out}}{V_{in\_rms} * pf * \eta} \qquad (1)$$

$$= \frac{6600}{230 * 0.95 * 0.93}$$

$$I_{in\_rms} = 32.5 \text{ A} \approx 33 \text{ A}$$

+25 % of rated current is considered as over current, then

$$I_{inrms} = 33 * 1.25 = 41.25 \text{ A}$$

$$I_{in\_rms} \approx 42 \text{ A}$$

+10 % ripple is considered in the maximum input current.

$$I_{ripple} = 10\% * 2 * \frac{P_{out}}{\sqrt{2} * V_{in\_rms} * pf * \eta} \qquad (2)$$

$$= 0.1 * \sqrt{2} * \frac{33}{2}$$

$$I_{ripple} = 2.333 \text{ A}$$

Then with the current ripple, filter inductances are given by the equation as follows:

$$L = \frac{V_{in} \times (V_o - V_{in})}{f_s \times I_{ripple} \times V_o} \qquad (3)$$

Since, V_{in} is varying. I_{ripple} is maximum when

$$V_{in} = \frac{V_o}{2}$$

Hence, we can write

$$L = \frac{V_{dc\_max}}{f_s \times I_{ripple} \times 4} \qquad (4)$$

$$= \frac{600}{100 * 1000 * 2.333 * 4}$$

$$L = 642.95 \ \mu\text{H}$$

+20 % margin is assumed for the inductor from the calculated value

Hence, filter inductance value is $L = 771.53 \ \mu\text{H}$

RMS current rating of the inductor is given as,

$$I_L = \frac{I_{in\_rms}}{2} \qquad (5)$$

$$I_L = 16.5 \ A$$

+30 % margin is assumed for the inductor value from the calculated value

$$I_L = 16.5 * 1.3$$

$$I_L = 21.45 \ A$$

$$I_L \approx 22 \ A$$

Therefore, filter inductors of $L = 780 \ \mu\text{H}$ is selected with current rating $I_L = 22$ A.

3.2 DC Link Capacitor Calculation

+5 % ripple is considered in the minimum output voltage.

$$V_{ripple} = 5\ \% * V_{dc\_min} \qquad (6)$$

$$V_{ripple} = 0.05 * 400$$

$$V_{ripple} = 20 \text{ V}$$

DC link capacitor value using ripple voltage is given as,

$$C \geq \frac{Pout}{2 * \pi * f_{grid} * V_{dc\_min} * V_{ripple}} \qquad (7)$$

DC link capacitor value using hold up time is given as,

$$C \geq \frac{P_{out} * t_{hold\_up}}{V_{ripple} * V_{dc\_nom}} \qquad (8)$$

Hold-up time is considered as 5 ms.

$$t_{hold\_up} = 5 \ ms$$

$$C = \frac{6600 * 5}{20 * 1000 * 450}$$

$$\text{C} = 3666.67 \ \mu\text{F}$$

Therefore, DC link capacitor of $C = 3700\ \mu F$ is selected with voltage rating 800 V.

4. Simulation and Results

The simulations of the on-board charger are carried out in MATLAB Simulink software. This section shows the simulations of the active front-end converter and the results obtained in the Simulink software.

4.1 Simulation Circuit

To validate the effectiveness of the designed controller and to check the performance of the AFC circuit, the selected AFC topology is simulated in MATLAB Simulink. Table.1 shows the components values considered for the MATLAB simulation of the circuit.

Table.1: Parameters of the AFC Circuit Considered for the MATLAB Simulations.

Parameters	Symbols	Values
AFC Inductors	L_1 and L_2	780 µH
AFC DC-link Capacitors	C	3700 µF
Switching Frequency	f_s	100 kHz
Sampling Frequency	F_s	100 kHz
Bandwidth of Current Controller	f_{cc_bw}	10 kHz
Bandwidth of Voltage Controller	f_{cv_bw}	5 Hz
Grid Voltage	V_g	230 V-rms
Grid Frequency	f_g	50 Hz
Power Rating of AFC	P_o	6600 W
Normal DC-link Voltage	V_{dc}	450 V

Fig.8 shows the AFC simulation circuit in grid-to-vehicle mode. The input to the AFC circuit in Fig.8 is 230 V, 50 Hz AC supply. the AFC converts AC supply to the form required by the batteries i.e., DC supply. Two reactors are used at the input to reduce the harmonics in the input supply and DC-link capacitor is used at load to decrease the ripples in the DC output of the AFC. The components values are designed in the previous section. The simulation results are used as the basis for hardware implementation.

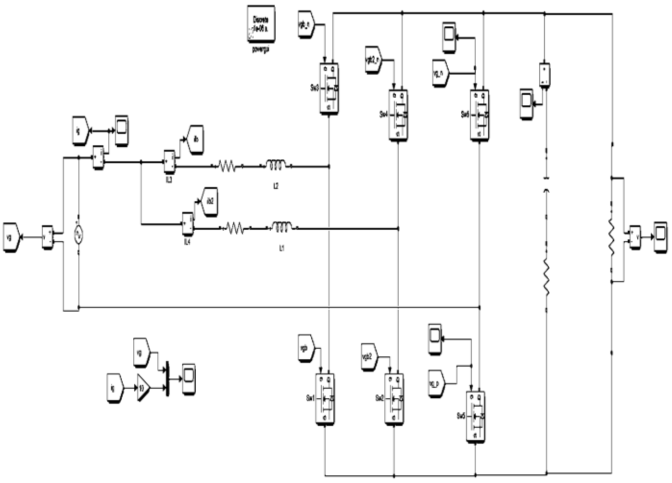

Fig.8: AFC Simulation Circuit in G2V Mode.

The practical AFC converter would always operate in CV mode, except during vehicle to load (V2L) mode. In voltage control mode, the dc-link voltage is regulated by the AFC and the current drawn from the grid would depend upon the load on the dc link. Hence, in the CV (constant voltage) mode, the reference current would be produced by the voltage controller.

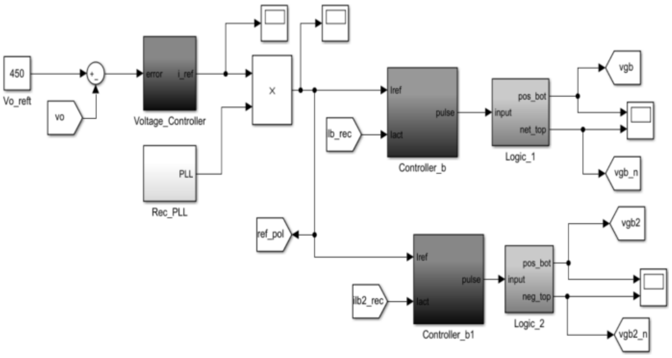

Fig.9: AFC Volatge Control Loop with Inner Current Control Loop.

The snapshot of the voltage control loop (at a high level) built-in MATLAB is shown in Fig.9. As seen, the rectified output of the PLL (i.e. rectified unit sine wave), which is in synchronous with the fundamental component of the grid frequency, is multiplied by the peak current reference value, which is generated by the voltage controller block.

4.2 Simulation Results

The results of the simulation circuits presented are included in the following section. The simulation results include the results of the AFC operation in current control mode and voltage control mode.

4.2.1 Current Control Mode

The switching pattern of all the switches G2V mode are shown in Fig.10. As seen in these figures, there is a deadtime of around 800 μs between the low-frequency pulses.

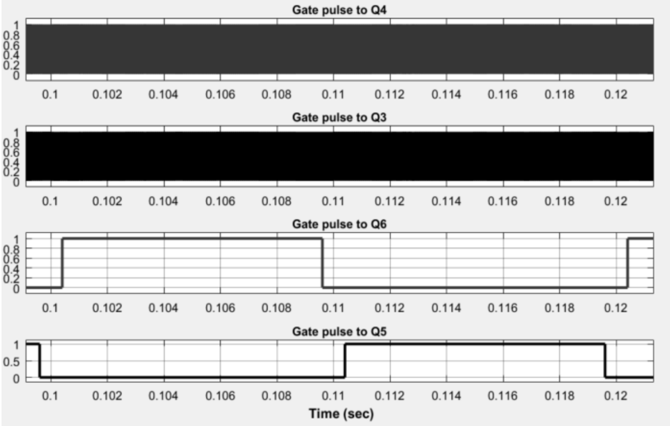

Fig.10: Switching Pattern of the Switches in AFC Circuit in G2V Mode.

The grid voltage (V_{grid} in Black) and scaled-up value of the grid current (10x in Red) for different values of current references are shown in Fig.11.

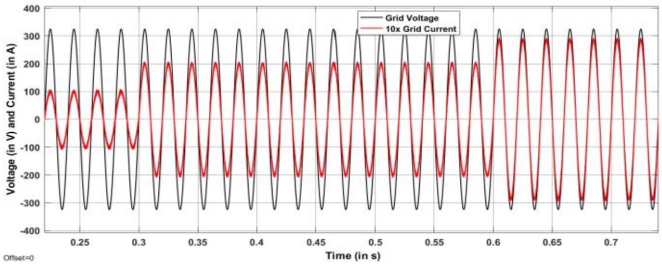

Fig.11: V_{grid} & I_{grid} in G2V Mode with a Different Values of the Inductor Current.

From Fig.10, it is noticed that the grid current follows the reference current with minimum overshoot and settling time. Furthermore, the results in Fig.11 successfully demonstrates the UPF operation.

The steady-state waveforms of grid voltage and current (two cycles of grid frequency) during G2V mode at rated condition (i.e. 6.6 kW) is shown in Fig.12.

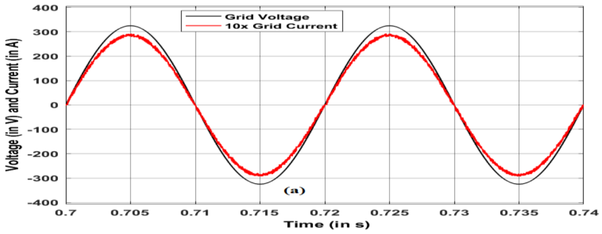

Fig.12: Steady-State Waveforms of the V_{grid} and I_{grid} at Rated Power Conditions During G2V Mode.

The simulations result of the AFC circuit in voltage control mode, where the dc-link voltage regulated by the AFC is as shown in Fig. 13.

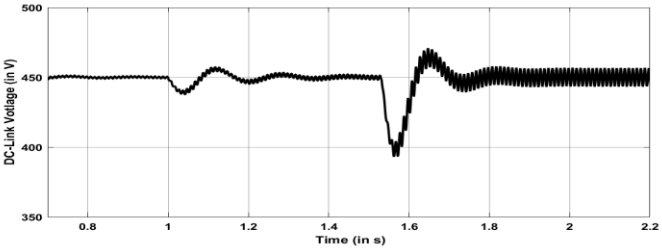

Fig.13: Simulation Result Showing dc-link Voltage with a Reference Value of 450V and Under Load Changing Conditions.

Also, from Fig.13, it is be inferred that voltage ripple in dc-link is limited to below 20V at rated conditions (i.e. at 6.6kW output power).

5. CONCLUSION

The active front-end converter with the aim to charge the electric vehicle battery of 6.6kW is designed. Bridgeless PFC converter is selected that reduces the number of semiconductor switches and also reduces the conduction losses. Totem-pole legs are interleaved so as to increase the overall efficiency and decrease the stress on the switches. The diodes are replaced by the semiconductor switches in order to obtain synchronous rectification. Overall, the converter implemented is totem-pole boost interleaved PFC converter. Converter is designed and simulations results are also shown. Results show the UPF operation of presented converter and the regulated output voltage at the desired value (450 V). The presented converter along with the DC-to-DC converter can be implemented in the design of OBC for EV. And this high efficiency electric vehicle can be used as immediate alternate solution for conventional vehicle.

REFERENCES

[1] N. Mars, F. Krouz, F. Louar and L. Sbita, "Comparison study of different dynamic battery model," *2017 International Conference on Green Energy Conversion Systems (GECS)*, Hammamet, 2017, pp. 1-6. doi: 10.1109/GECS.2017.8066241

[2] M. A. Hannan, M. M. Hoque, A. Hussain, Y. Yusof and P. J. Ker, "State-of-the-Art and Energy Management

System of Lithium-Ion Batteries in Electric Vehicle Applications: Issues and Recommendations," in *IEEE Access*, vol. 6, pp. 19362-19378, 2018. doi: 10.1109/ACCESS.2018.2817655

[3] N. Sakr, D. Sadarnac and A. Gascher, "A review of on-board integrated chargers for electric vehicles," *2014 16th European Conference on Power Electronics and Applications*, Lappeenranta, 2014, pp. 1-10. doi: 10.1109/EPE.2014.6910865

[4] A. Emadi, S. S. Williamson and A. Khaligh, "Power electronics intensive solutions for advanced electric, hybrid electric, and fuel cell vehicular power systems," in *IEEE Transactions on Power Electronics*, vol. 21, no. 3, pp. 567-577, May 2006. doi: 10.1109/TPEL.2006.872378

[5] J. G. Kassakian, "Automotive electrical systems-the power electronics market of the future," *APEC 2000. Fifteenth Annual IEEE Applied Power Electronics Conference and Exposition (Cat. No.00CH37058)*, New Orleans, LA, USA, 2000, pp. 3-9 vol.1. doi: 10.1109/APEC.2000.826075

[6] F. Musavi, W. Eberle and W. G. Dunford, "A High-Performance Single-Phase Bridgeless Interleaved PFC Converter for Plug-in Hybrid Electric Vehicle Battery Chargers," in *IEEE Transactions on Industry Applications*, vol. 47, no. 4, pp. 1833-1843, July-Aug. 2011. doi: 10.1109/TIA.2011.2156753